The Impedance Properties Analysis of Composite Electrodes for Supercapacitor

Jin-Yan Song
School of Information Engineering
Dalian Ocean University
Dalian, China
thesjyyan@163.com

Teng Gao
School of Mechanical Engineering & Automation
Dalian Polytechnic University
Dalian, China
gaoteng@dlpu.edu.cn

Dalian, China
miaoxinying@dlou.edu.cn
haoliying@dlou.edu.cn
caikewei@dlou.edu.cn

Xin-Ying Miao, Li-ying Hao,Ke-wei Cai
School of Information Engineering
Dalian Ocean University

Abstract—**Supercapacitor can get high energy density and the ability of quick charging and discharging. In this work, the different mass ratios of composite electrodes mixed with active carbon (AC) based on $RuO_2 xH_2O$, were prepared to study the electrical performance parameters of the incorporations. Through Conway's model and impedance spectroscopy, the composite electrode model has been established, and it is validated by the experiments on their electrochemical performances for different proportions of composite electrodes fabricated with $RuO_2 xH_2O$ and active carbon. The simulation results show that the composite electrode with 60wt.% amorphous hydrous ruthenium oxide has the lower inner resistance and the higher degree of ruthenium oxide utilization, which are testified by the experiments.**

Keywords- Supercapacitor; Impedance; Spectroscopy; Equivalent Circuit Model; Mass Ratio

I. INTRODUCTION

Supercapacitors are widely used in pulse power source as energy storage element, due to their high-power density, long cycle life, and bridging function for the power/energy gap between traditional dielectric capacitors (which have been high-power output) and batteries/fuel cells (which have been high-energy storage)[1-3]. Currently, the electrode material research concentrated on the carbons [4-7], the transition metal oxide [8-10] and conducting polymers [11-13], which all have high specific capacitance in the electrolyte. Transition metal oxides such as ruthenium oxide [14, 15], manganese oxide [16], cobalt oxide [9], and nickel oxide [17], which have drawn extensive research attention as electrode materials, are qualified to be electrode materials for electrochemical capacitor. Ruthenium oxide exhibits excellent properties as pseudo-capacitive electrode materials. However, the expensive price restricts its wider applications [18]. In the ruthenium oxide mixed with other types of electrode materials is a commonly used method. As Mn [15], carbon [19], and Ti [20], and other types of electrode materials [21, 22] are incorporated in a common method of ruthenium oxide. So in the ruthenium oxide with these materials, the material quality in the whole electrode ratio on the electrical performance parameters of the electrode what effect? In this paper, the problem has been solved by established the equivalent circuit models, the element parameters of which were extracted by impedance spectroscopy. The different mass ratios $RuO_2 xH_2O/AC$ composite electrodes have been prepared to obtain associated electrical properties of experimental parameters. Through simulation and experimental results, we obtain the relationships between the resistance and capacitance change with the mass ratio, the density and other basic parameters of the composite electrodes, such as to prepare corresponding composite electrodes in the different applications.

II. EXPERIMENTS

A. Preparation of the electrodes and the samples

The hydrous ruthenium oxide powder was formed by a Sol-gel process. Then hydrous ruthenium oxide and active carbon powder at the mass ratio α of hydrous ruthenium oxide in the composite electrodes mixed and skived equability that adding to the proper PTEF. According to the membrane preparation technology, pressed them into the thickness of 0.2mm membrane, intercepted the dimension of $1 \times 1 cm^2$ membranes and pressed it on the tantalum foil current collectors. Then the two above uniform electrodes are separated by the fiberglass cloth, infused in the concentration of 38% vitriol electrolyte to compose of the symmetrical super-capacitor unit as the samples. When the mass ratio of hydrous ruthenium oxide in the composite electrodes α=0, 0.1, 0.2, 0.3, 0.4, 0.5, 0.6, 0.7, 0.8, 0.9, 1.0, it fabricates 11 super-capacitors of the same thickness.

B. The Performance Test of Composite Electrodes

The equipment used in the experiments is mainly CHI660A model electrochemistry workstation. The experiment temperature is room temperature.

Charging and discharging test are made for the above samples, the constant current of charging and discharging is 3mA, the range of charge and discharge voltage is 0-1V. According to the measured charge and discharge curve, it can obtain the specific capacitance of the composite electrodes:

Where I is the discharging current; $\triangle t$ and $\triangle V$ are the time difference and voltage difference of corresponding discharging process respectively; C_p is the specific capacitor of single electrode in F/g; m is the average mass of two electrodes of super-capacitors.

Added a small magnitude sine AC signal on above samples with the frequency of 0.1Hz ~ 100 kHz and the voltage of 5mV, measurement results can be gotten from Electrical Impedance Spectroscopy (EIS)

III. MODELLING OF COMPOSITE ELECTRODES FOR SUPER-CAPACITORS

Using kinetic parameters to create a supercapacitor equivalent circuit model is one of the main EIS analyses; it can compare the performance of the electrode kinetics intuitively [25]. At present, the common supercapacitor models mainly have a simple model of the ESR [26], Conway's model [27], transmission line model [28] and neural network model [29], etc. This article used the Conway's model to establish the model of the composite electrodes.

Conway established the equivalent circuit model of super-capacitor, as seen in Fig.1, where $R\Omega$, R_s, C_d and C_s represent lead and electrolyte resistance, rate constant, double layer capacitance and Faraday capacitance, respectively. The real part and imaginary part of impedance Z_i, Z_j are respectively given by:

$$Z_i = R_\Omega + \frac{R_s}{(1+\frac{C_d}{C_s})^2 + (\omega C_d R_s)^2} \tag{1}$$

$$\text{and } Z_j = \frac{\frac{1}{\omega C_s}(1+\frac{C_d}{C_s}) + \omega C_d R_s^2}{(1+\frac{C_d}{C_s})^2 + (\omega C_d R_s)^2} \tag{2}$$

Here ω is angle frequency. Capacitance can be calculated by:

$$C(\omega) = \text{Re}\,\underline{C} = \frac{\text{Im}Y}{\omega} = \frac{-\text{Im}Y}{\omega|Z|^2} = \frac{-\text{Im}Z}{\omega[(\text{Re}\,Z)^2 + (\text{Im}\,Z)^2]} \tag{3}$$

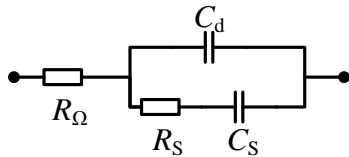where Z, Y and $\underline{C}$ is the impedance, admittance and the complex capacitance, respectively.

Figure 1.   The Conway's model for supercapacitor

For RuO$_2$ xH$_2$O/active carbon composite electrodes, when $\alpha=0$, it is pure active carbon electrode. The real

part and imaginary part of impedance can be expressed in terms of Fig.1 as:

$$Z_{iC} = R_{\Omega C} + \frac{R_{sC}}{(1+\frac{C_{dC}}{C_{sC}})^2 + (\omega C_{dC} R_{sC})^2} \tag{4}$$

$$\text{and } Z_{jC} = \frac{\frac{1}{\omega C_{sC}}(1+\frac{C_{dC}}{C_{sC}}) + \omega C_{dC} R_{sC}^2}{(1+\frac{C_{dC}}{C_{sC}})^2 + (\omega C_{dC} R_{sC})^2} \tag{5}$$

where $R\Omega C$, ZiC, ZjC, RsC, CdC and CsC are the lead and electrolyte resistance, real impedance, imaginary impedance, double layer capacitance and Faraday capacitance of active carbon electrodes, respectively.

When $\alpha=1$, it is pure RuO2 xH2O electrode. The real part and imaginary part of impedance are obtained from the following equations, respectively.

$$Z_{iRu} = R_{\Omega Ru} + \frac{R_{sRu}}{(1+\frac{C_{dRu}}{C_{sRu}})^2 + (\omega C_{dRu} R_{sRu})^2} \tag{6}$$

$$\text{and } Z_{jRu} = \frac{\frac{1}{\omega C_{sRu}}(1+\frac{C_{dRu}}{C_{sRu}}) + \omega C_{dRu} R_{sRu}^2}{(1+\frac{C_{dRu}}{C_{sRu}})^2 + (\omega C_{dRu} R_{sRu})^2} \tag{7}$$

Here $R\Omega Ru$, $ZiRu$, $ZjRu$, $RsRu$, $CdRu$ and $CsRu$ are the lead and electrolyte resistance, real impedance, imaginary impedance, double layer capacitor and Faraday capacitor of pure RuO2 xH2O electrodes, respectively.

The super-capacitor made in RuO2 xH2O/C composite electrodes at $\alpha=0\sim1$ also satisfies the model in Fig.1. As the active carbon and RuO2 xH2O particulate in the process do not affect their properties, RuO2 xH2O and active carbon do not influence each other. The electrolyte concentration is assumed to be invariant and side reactions and thermal effects are ignored, the electrolyte resistance is invariant. To remove the part of electrolyte resistance, the equivalent circuit of composite electrodes could be seen as two capacitors of pseudo-capacitor from RuO2 xH2O and double layer capacitor from active carbon in parallel. Therefore the equivalent circuit can be seen in Fig.2, where $R\Omega f$, $Rsfc$ and $RsfRu$, CdC and $CdfRu$, $CsfC$ and $CsfRu$ are lead and electrolyte resistance of composite electrodes, rate constant of active carbon and RuO2 xH2O, double layer capacitors and pseudo-capacitors of active carbon and RuO2 xH2O, respectively. From Fig.2, it can be seen that the resistance and reactance of the first and second branch are separately written as:

$$Z'_{ifc} = \frac{R_{sfC}}{(1+\frac{C_{dfC}}{C_{sfC}})^2 + (\omega C_{dfC} R_{sfC})^2} \tag{8}$$

$$\text{and } Z'_{jfc} = \frac{\frac{1}{\omega C_{sfC}}(1+\frac{C_{dfC}}{C_{sfC}}) + \omega C_{dfC} R_{sfC}^2}{(1+\frac{C_{dfC}}{C_{sfC}})^2 + (\omega C_{dfC} R_{sfC})^2} \cdot \tag{9}$$

The resistance and reactance of the third and fourth branch are separately expressed as:

$$Z'_{ifRu} = \frac{R_{sfRu}}{(1+\frac{C_{dfRu}}{C_{sfRu}})^2 + (\omega C_{dfRu} R_{sfRu})^2} \quad (10)$$

$$\text{and } Z'_{jfRu} = \frac{\frac{1}{\omega C_{sfRu}}(1+\frac{C_{dfRu}}{C_{sfRu}}) + \omega C_{dfRu} R_{sfRu}^2}{(1+\frac{C_{dfRu}}{C_{sfRu}})^2 + (\omega C_{dfRu} R_{sfRu})^2} \quad (11)$$
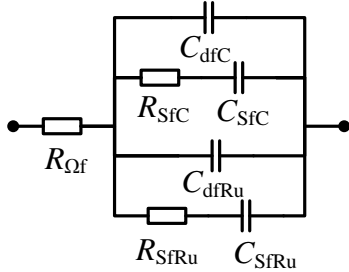

Figure 2.   The equivalent circuit for supercapacitor composed of composite electrodes

It is known that $R_s = R_{ct} + \frac{\sigma}{\sqrt{\omega}}$, $R_{ct} = \frac{RT}{nFi_o}$, $C_s = \frac{1}{\sigma\sqrt{\omega}}$,

$\sigma = \frac{1}{nFA\sqrt{2}}(\frac{\beta_{ox}}{\sqrt{D_{ox}}} - \frac{\beta_{rd}}{\sqrt{D_{rd}}})$, $\beta_{ox} = \frac{RT}{nFC_{ox}^b}$, $\beta_{rd} = -\frac{RT}{nFC_{rd}^b}$,

$i_o = nFAk(C_{ox}^b)^{1-\alpha}(C_{Rd}^b)^{\alpha}$

Where Rct: charge transmission resistance; n: charge shift number; F: Faraday constant; i0: transfer current; Coxb and Crdb are the oxide and the reducer concentration of the solution. Due to the area and thickness of each electrode are uniform, the electrolyte concentration is steady and the oxide and reducer concentrations of the solution are steady, βox, βrd, Dox, Drd can be seen as constant. If the variation of the double layer capacitance is along with potential, the double layer capacitance is proportion to the electrode area. It is supposed that the electrode thickness is d, the electrode area is A, the area of RuO2 xH2O in composite electrode is AfRu, the area of active carbon in composite electrode is AfC, the density of RuO2·xH2O and active carbon are ρRu, ρC. It can be obtained from the following two equations, respectively.

$$\frac{R_{ctC}}{R_{ctfC}} = \frac{\sigma_{ctC}}{\sigma_{ctfC}} = \frac{C_{sfC}}{C_{sC}} = \frac{C_{dfC}}{C_{dC}} = \frac{A_{fC}}{A} = \frac{(1-\alpha)\rho_{Ru}}{(1-\alpha)\rho_{Ru} + \rho_C \alpha} \quad (12)$$

$$\frac{R_{ctRu}}{R_{ctfRu}} = \frac{\sigma_{ctRu}}{\sigma_{ctfRu}} = \frac{C_{sfRu}}{C_{sRu}} = \frac{C_{dfRu}}{C_{dRu}} = \frac{A_{fRu}}{A} = \frac{\alpha\rho_C}{(1-\alpha)\rho_{Ru} + \alpha\rho_C} \quad (13)$$

Because the areas and thicknesses of composite electrodes are uniform, it can be supposed that the electrolyte resistances of composite electrodes is same, namely RΩf＝RΩc＝RΩRu. It can be reduced that the impedances of the active carbon and RuO2 xH2O of composite electrodes are respectively the proportion to the pure active carbon and RuO2 xH2O electrodes. Submitting (12) and (13) into (8)~(11):

$$\frac{Z'_{ifc}}{Z_{ic} - R_\Omega} = \frac{Z'_{ifc}}{Z'_{ic}} = \frac{Z'_{jfC}}{Z_{jC}} = \frac{A_{fC}}{A} \quad (14)$$

$$\text{and } \frac{Z'_{ifRu}}{Z_{iRu} - R_\Omega} = \frac{Z'_{ifRu}}{Z'_{iRu}} = \frac{Z'_{jfRu}}{Z_{jRu}} = \frac{A_{fRu}}{A} \quad (15)$$

Therefore, the resistance and reactance of composite electrodes can be obtained by the following two equations, respectively:

$$Z_{if} = R_\Omega + \frac{[(1-\alpha)\rho_{Ru} + \rho_C\alpha]^2 Z'_{ic} Z'_{iRu}}{[(1-\alpha)\alpha\rho_{Ru}\rho_C + \rho_C^2\alpha^2]Z'_{ic} + [(1-\alpha)\alpha\rho_{Ru}\rho_C + (1-\alpha)^2\rho_{Ru}^2]Z'_{iRu}} \quad (16)$$

and

$$Z_{jf} = \frac{[(1-\alpha)\rho_{Ru} + \rho_C\alpha]^2 Z_{jC} Z_{jRu}}{[(1-\alpha)\alpha\rho_{Ru}\rho_C + \rho_C^2\alpha^2]Z_{jC} + [(1-\alpha)\alpha\rho_{Ru}\rho_C + (1-\alpha)^2\rho_{Ru}^2]Z_{jRu}} \quad (17)$$

In terms of (3), (16), (17), it can deduce the relationships α with real resistance, imaginary impedance and capacitance.

IV.   RESULTS AND DISCUSSION

In order to review the variety of resistance and capacitance of super-capacitors at different ratios α, it need to measure the Impedance Spectroscopy of the super-capacitors fabricated with pure active carbon and pure RuO2 xH2O electrodes, respectively, as seen in Fig.3 curve A, F. In order to observe the variety rule of inner resistances of super-capacitor with α, it is observed that the change curve of real resistance by (16) at 1.758×10^4Hz, $Z_j\approx0$; The repeat frequency of charge and discharge used in pulse power source is usually around 0-100Hz, so it selects the resistance of super-capacitor at f=1Hz and calculated the variety rule of capacitances of composite electrodes at different ratios α by (3). Table.I is the data involved in models parameters in equations.
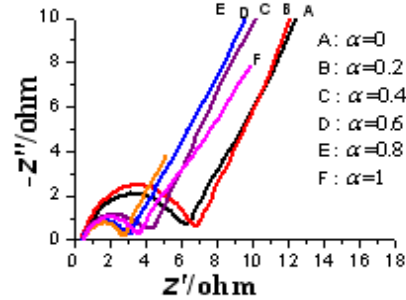

Figure 3.   Impedance characteristics of composite electrodes

TABLE I.   PARAMETERS THAT DESCRIBE THE COMPOSITE ELECTRODE

Parameter	Value	Ref.
RΩ	0.3Ω	Assumed
ρC	1.09g/cm3	Factory
ρRu	0.5g/cm3	measured
Zic(f=1Hz)	0.7586Ω	measured
ZiRu(f=1Hz)	0.3987 Ω	measured
Zjc (f =1Hz)	-1.8120Ω	measured
ZiRu (f =1Hz)	-0.8882Ω	measured
Zic (f =1.76×104Hz)	0.3819Ω	measured
ZiRu(f =1.76×104Hz)	0.4872Ω	measured

In Fig.4 the solid line is relationship of $Z'_{if}(\omega)$ calculated by (14) and α at 1.758×10^4Hz; the dot is the resistances at different ratios α at 1.758×10^4Hz. From the simulation results, in α = [1, 0.6], $Z'_{if}(\omega)$ descends rapidly and the resistance of composite electrodes changes evidently; In the range of [0.6, 0], $Z'_{if}(\omega)$ drops slowly, the

change is not big. It is obvious that in the range [0.6, 1] reducing the resistance of electrodes has obvious effect. From Fig.3, the above result is also proved, we can see, that after adding to the active carbon, the inner resistance of super-capacitor minishes along with the α, Faraday impedance circularity of pure RuO_2 xH_2O is smaller than of pure active carbon, namely charge transmission resistance R_{ct} of pure RuO_2 xH_2O is smaller than of pure active carbon, but when $\alpha = 0.4$, 0.6, 0.8, Faraday resistance circularity of them is smaller than of pure RuO_2 xH_2O. It shows that pore active carbon adhere to RuO_2 xH_2O after adding to active carbon, the pores of electrodes and the electrolyte inside the pores of the electrodes increases, as a result the contact resistant between the particles of electrodes minishes to decrease the inner resistance of composite electrodes. On the other hand, when the proportion of the active carbon is not big, as the ions of electrolyte inside the pores of the electrodes is in favor of the transmission of the charge and the concentration of reactant increases, the charge transmission resistance decreases, but when the proportion of active carbon is bigger than a certain value, active carbon of the electrodes takes the main action to increase the charge transmission resistance.
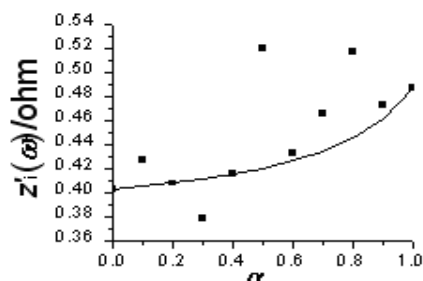

Figure 4. At 1.76×104Hz, the relation of Z'i(ω) and α: the solid line is the simulation data, the dots is the actual data

In Fig.5, the solid line is the calculated relationship of $C(\omega)$ and α at 1Hz; the dot is the measured data at 1Hz at different α. As seen in Fig.5, $C(\omega)$ approximately minishes linearly along with increasing the active carbon. When $\alpha = 0$, 0.2, 0.4, 0.6, 0.8, 1, the discharge curve of composite electrodes at 3mA constant current can be seen in Fig.6. In terms of the calculated equation, the specific capacitances are respectively: 131F/g, 230F/g, 345F/g, 567F/g, 667F/g, 776 F/g, and when α=0.1, 0.3, 0.5, 0.7, and 0.9 that cannot be seen in Fig.5, the specific capacitances are: 160F/g, 289F/g, 436F/g, 587F/g and 692F/g. For the variety of specific capacitance, it shows that when the content of RuO_2 xH_2O is low, the grains of RuO_2 xH_2O are almost covered by the particles of active carbon, and composite electrodes represent the nature of active carbon; When the content of RuO_2 xH_2O increase gradually, the effects of RuO_2 xH_2O strengthen. For the capacitance of RuO_2 xH_2O is decuple higher than that of active carbon, the specific capacitance of composite electrodes increase rapidly along with increasing the content of RuO_2 xH_2O.

Therefore, it can be seen that the RuO_2 xH_2O mass ratio of composite electrode $\alpha = 0.6$ is perfect from the results of the simulation and experiments, that minishes the inner resistance as ensuring the high specific capacitance.
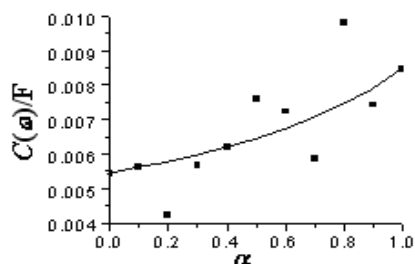

Figure 5. At 1Hz, the relation of C(ω) and α: the solid line is the simulation data, the dots is the actual data
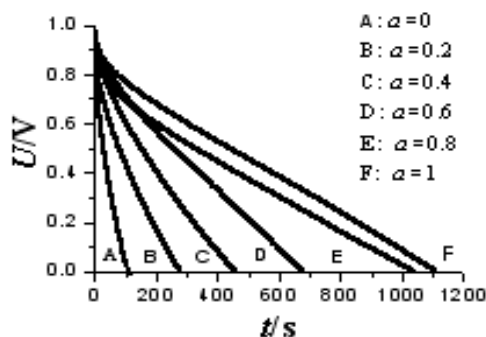

Figure 6. Discharge curves of composite electrodes

V. CONCLUSION

In this paper, RuO2 xH2O/active carbon composite electrodes for hybrid super-capacitor is studied. The relationships of the resistance and capacitance with the mass ratio α of RuO2 xH2O in the composite electrode that is made of RuO2 xH2O powder and active carbon, is analyzed. The simulation and experiment results show that adding active carbon into RuO2 xH2O can improve the impedance of composite electrodes, but reduce the specific capacitance. Considered the above aspects, when the mass ratio of ruthenium oxide is about 60%, the specific capacitance of composite electrodes is 567F/g and the inner resistance is 0.4331Ω.

REFERENCES

[1] D.H. Seo, Z.J. H, S. Kumar and K. Ostrikov, "Structure-Controlled, Vertical Graphene-Based, Binder-Free Electrodes from Plasma-Reformed Butter Enhance Supercapacitor Performance," Adv. Energy Mater, vol. 3, 2013, pp. 1316-1323.

[2] P. Sharma and T.S. Bhatti, "A review on electrochemical double-layer capacitors," Energy Conversion and Management, vol. 51, 2010, pp. 2901-2912.

[3] K. Wang, L. Zhang, B.C. Jin, and J.L. Yuan, "The thermal analysis on the stackable supercapacitor," Energy, vol. 59, 2013, pp. 440-444.

[4] M. Beidaghi and Y. Gogotsi, "Capacitive energy storage in micro-scale devices:recent advances in design and fabrication of microsupercapacitors," Energy & Environmental Science, vol. 7, 2014, pp. 867-5-884.

[5] K. Wang, C. L, B.C. Ji, " Preparation of electrode Based on Plasma Modification and its Electrochemical Application," Journal of Materials Engineering and Performance, vol. 23, 2014, pp. 588-592.

[6] K. Wang and L. Zhang, "Synthesis of ordered mesoporous carbon and its electrochemical performances," International Journal of Electrochemical Science, vol. 8, 2013, pp. 2892-2897.

[7] Z.Q. Dai, K. Wang, L.W. Li and T.Z. Zhang, "Synthesis of nitrogen-doped graphene with microwave," International Journal of Electrochemical Science, vol. 8, 2013, pp. 9384-9389.

[8] W. Yang, Z. Gao, J. Ma, X.M. Zhang, J. Wang and J.Y. Liu, "Hierarchical NiCo2O4 @ NiO core–shell heterostructured nanowire arrays on carbon cloth for a high-performance flexible all-solid-state electrochemical capacitor," Journal of Materials Chemistry, vol. 2, 2014, pp. 1448-1457.

[9] J. Xu, Q. Wang, X. Wang, Q.Y. Xiang, B. Liang, D. Cheng and G.Z. Shen, "Flexible Asymmetric Supercapacitors Based upon Co9S8 Nanorod//Co3O4 @ RuO2 Nanosheet Arrays on Carbon Cloth," ACS Nano, vol. 7, 2013, pp. 5453-5462.

[10] K. Wang, L. Li and T. Zhang, "Synthesis of nickel hydroxide and its electrochemical performances," International Journal of Electrochemical Science, vol. 8, 2013, pp. 6252-6257.

[11] C. Zhou, Y.W. Zhang, Y.Y. Li and J.P. Liu, "Construction of High -Capacitance 3D CoO @ Polypyrrole Nanowire Array Electrode for Aqueous Asymmetric Supercapacitor," Nano Letter, vol. 13, 2013, pp. 2078-2085.

[12] K. F. Babu, S. P. Siva Subramanian and M. A. Kulandainathan, "Functionalisation of fabrics with conducting polymer for turning capacitance and fabrication of supercapacitor," Carbohydrate Polymers, vol. 94, 2013, pp. 487-495.

[13] C. Zhou, Y.W. Zhang, Y.Y. Li and J.P. Liu, "Construction of High-capacitance 3D CoO@Polypyrrole Nanowire Array Electrode for Aqueous Asymmetric Supercapacitor," Nano Letter, vol. 13, 2013, pp. 2078–2085.

[14] K.M. Kim, J.H. Nam, Y.G. Lee, W.L. Cho and J.M. Ko, "Supercapacitive properties of electrodeposited RuO2 electrode in acrylic gel polymer electrolytes," Current Applied Physics, vol. 13, 2013, pp. 1702-1706.

[15] L. Zhang, J.Y. Song, and J.Y. Zou, "Electrochemical Property of Ru-Mn-AC Multi-Element Composite Electrode Materials," Rare Metal Materials and Engineering, vol. 38, 2009, pp. 11-14.

[16] H. Ashassi-sorkhabi, E. Asghari and P. Badakhshan, "Potentiostatic and cyclic voltammetric deposition of nanostructured manganese oxide for supercapacitor applications," Current Applied Physics, vol. 14, 2014, pp. 187-191.

[17] K. Wang, L. Zhang, Y.H. Jin and Y. Fan, "The preparation of nickel oxide based on infinite dilute method and its electrochemical performance," Russian Journal of Electrochemistry, vol. 50, 2014, pp. 192-196

[18] H.T. Fang, M. Liu, D.W. Wang, X.H. Ren and X. Sun, "Fabrication and supercapacitive properties of a thick electrode of carbon nanotube‑RuO2 core‑shell hybrid material with a high RuO2 loading," Nano Energy, vol. 2, 2013, pp. 1232-1241.

[19] K. Wang, L. Li and X.Wu, "Synthesis of active carbon and ruthenium oxide for electrochemical performance," International Journal of Electrochemical Science, vol. 8, 2013, pp. 6574-6578.

[20] P.C. Chen, S.J. Hsieh, J. Zou, and C.C. Chen, "Selectively dealloyed Ti/TiO2 network nanostructures for supercapacitor application," Materials Letters, vol. 133, 2014, pp. 175-178.

[21] X. Liu, J. Zhu, X. Wang, J. Sun, Z. Tang, T. Zhang and M.J.O, "Capacitive Properties and Structure of RuO2-HfO2 Films Prepared by Thermal Decomposition," Method.Physics Procedia, vol. 50, 2013, pp. 416-420.

[22] S.N. Pusawale, P.R. Deshmukh, J.L. Gunjakar and C.D. Lokhande, "SnO2-RuO2 composite films by chemical deposition for supercapacitor application," Materials Chemistry and Physics, vol. 139, 2013, pp. 416-422.

[23] J.Y. Zou, L. Zhang and J.Y. Song, "Development of the 40V Hybrid Supercapacitor Unit," IEEE transation on magnetics, vol. 41, 2005, pp. 294-298.

[24] J.Y. Song, L. Zhang and Z.J. Zou, "Investigations on Increasing the Operation Voltage of Hybrid Supercapacitors used in Pulsed Power System," 18th IEEE PPC, 2011, pp. 717-720.

[25] S. Faraji and F.N. Ani, "Microwave-assisted synthesis of metal oxide/hydroxide composite electrodes for high power supercapacitors - A review", Journal of Power Sources, vol. 263, 2014, pp. 338-360.

[26] V. Barsukov and S. Chivikov, "The "capacitor" concept of the current-producing mechanism in polyaniline-type conducting polyers," Electrochimica Acta, vol 41, 1996, pp. 1773-1779

[27] R.P. Simpraga and B.E. Conway, "The real-area scaling factor in electrocatalysis and in charge storage by supercapacitors," Electrochimica Acta, vol. 43, 1998, pp. 3045-3058.

[28] K. Wang, L. Zhang, B. Ji and J. Yuan, "The thermal analysis on the stackable supercapacitor," Energy, vol. 59, 2013, pp. 440-444.

[29] A. Eddahech, O. Briat, M. Ayadi and J.M. Vinassa, "Modeling and adaptive control for supercapacitor in automotive applications based on artificial neural networks," Electric Power Systems Research, vol. 106, 2014, pp. 134-141.